JOURNAL OF VIROLOGY, Aug. 1996, p. 5422–5429 Vol. 70, No. 8
0022-538X/96/$04.00+0

Identification of Domains in Canine Parvovirus VP2 Essential for the Assembly of Virus-Like Particles

ALICIA HURTADO,[1] PALOMA RUEDA,[1] JANE NOWICKY,[2] JAVIER SARRASECA,[1] AND J. IGNACIO CASAL[1]*

Inmunologia y Genética Aplicada S.A., 28037 Madrid, Spain,[1] and State Veterinary Institute for Virus Research, Lindholm, DK-4771 Kalvehave, Denmark[2]

Received 20 February 1996/Accepted 1 May 1996

Canine parvovirus capsids are composed of 60 copies of VP2 and 6 to 10 copies of VP1. To locate essential sites of interaction between VP2 monomers, we have analyzed the effects of a number of VP2 deletion mutants representing the amino terminus and the four major loops of the surface, using as an assay the formation of virus-like particles (VLPs) expressed by recombinant baculoviruses. For the amino terminus we constructed three mutants with progressively larger deletions, i.e., 9, 14, and 24 amino acids. Deletions of 9 and 14 amino acids did not affect the morphology and assembly capabilities of the mutants. However, the mutant with the 24-amino-acid deletion did not show hemagglutination properties or correct VLP morphology, stressing again the relevance of the RNER domain in canine parvovirus functionality. Three of the four mutants with deletions in the loops failed to make correct VLPs, indicating that these regions are essential for correct capsid assembly and morphology. Only the mutant with the deletion in loop 2 was able to assemble in regular VLPs, suggesting that this loop has little or no effect in capsid morphogenesis. Further research has demonstrated that this region can tolerate the insertion of foreign epitopes that are correctly exposed in the surface of the capsid. This result opens the door to the use of these VLPs for antigen delivery.

Canine parvovirus (CPV) is a member of the *Parvovirus* genus. CPV particles have a diameter of 25 nm and are composed of three proteins, VP1, VP2, and VP3. VP2 is the major component of the viral capsid and contains 584 amino acid residues. Each particle contains around 60 copies of VP2 and between 6 and 10 copies of VP1. In the infectious particles some VP2 is processed proteolytically to VP3. CPV capsids are composed of a core structure comprising an eight-stranded antiparallel β-barrel motif present in most other known icosahedral viruses (17), with four large loops between several strands of the β-barrel (24). Loops 3 and 4 are usually grouped as the long GH loop. Loops 1, 3, and 4 from three different VP2 molecules are in close proximity, suggesting extensive interactions between threefold-related subunits. These subunits are highly intertwined with one another, forming a 22-Å (2.2-nm)-long protrusion on the threefold axes (the spike), which contains most of the residues related to the antigenic properties of the virus (21). The four loops make up much of the surface of the virus capsid and comprised about 364 of the 547 residues resolved in the VP2 structure. In contrast, the N-terminal 37 residues of VP2 are barely visible, presumably because of its disordered nature. It has been suggested that a few of the amino termini run along the fivefold axis to the exterior of the capsid. Another important antigenic region has been located in this amino terminus (4, 12, 13, 15).

The structure of the loops determines many of the properties of the virus. From an antigenic point of view, two major neutralization sites have been defined in these loops (21). Site A comes from loops 1 and 2 of one VP2 and loop 4 of a threefold-related molecule. The role of loop 2 in the formation of this epitope was shown by the effect of mutations of residues 222 and 224. Site A is also implicated in the antigenic drift from CPV type 2a to 2b through residue 426 in loop 4. Site B involves residues 299, 300, and 302 on the shoulder of the threefold spike, in the extended portion of loop 3. In fact, residue 300 is the most variable residue in CPV. Monoclonal antibodies (MAbs) that recognize these two determinants efficiently inhibited hemagglutination (HA) (21). However, these changes did not affect in vivo cross-protection.

Some changes in residues 298, 299, 300, and 301 of loop 3 are also related to the loss of the ability of CPV to replicate in canine cells (23), and changes in residues 316 and 320 are related to the changes necessary to allow minute virus of mice MVM(i) to grow in fibroblasts like MVM(p) (1). Residues 323 and 375 are involved in the pH dependence of HA (5). Also, the regions on the shoulder of the threefold spike or in the twofold depression have been implicated in receptor attachment (6). Finally, most of the changes in the pathogenicity of some parvoviruses, such as Aleutian disease virus, are associated to the disordered N-terminal section, although some other changes have been located in loop 1, which extends from the canyon, and in the exposed part of loop 2 (2).

We have developed a system that allows us to study the effects of different domains and residues of VP2 in the interactions necessary for the assembly of the capsid. Expression of CPV VP2 in insect cells results in the assembly of virus-like particles (VLPs), which indicates that VP2 alone is sufficient for capsid assembly (14, 18). Our studies on CPV VP2 have involved the synthesis of a series of mutants with internal deletions in the four major loops of the surface of the capsid. In addition, and given the relevance of the amino terminus, we have prepared several mutants with deletions in this terminus. From these studies, we have identified several regions in the amino terminus and in loops 1, 3, and 4 that appear to be essential for VLP formation. Also, permissive sites for deletion in loop 2 and in the amino terminus have been identified. These sites might be useful for the construction of CPV chimeric particles containing foreign epitopes.

* Corresponding author. Present address: Inmunologia y Genética Aplicada S.A. (INGENASA), Hnos. Garcia Noblejas 41, 2°, 28037 Madrid, Spain. Phone: 34 1 3680501. Fax: 34 1 4087598. Electronic mail address: INGENASA@alc.es.

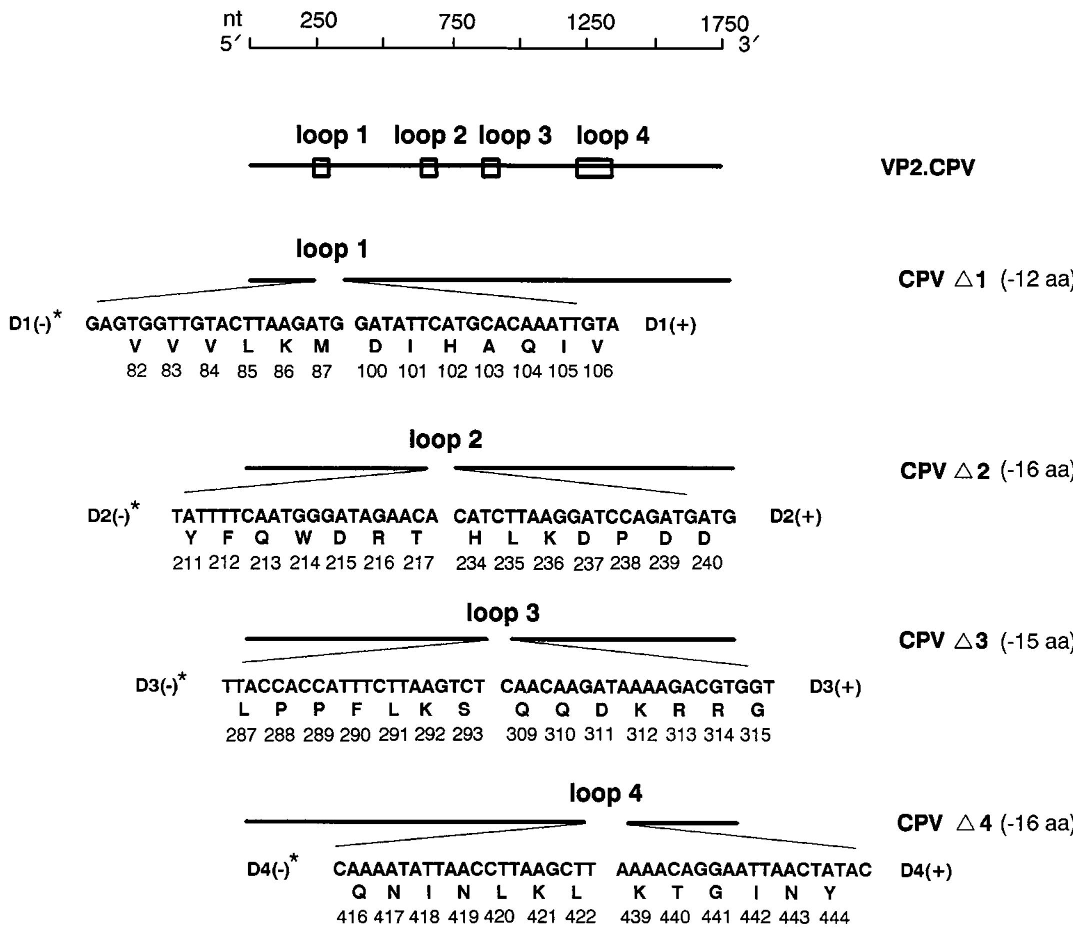

FIG. 1. Diagrams of CPV VP2 deletion mutants Δ1 to Δ4. The CPV VP2 diagram at the top represents the positions of the loops with respect to the nucleotide sequence. The other diagrams represent the deletion mutants of VP2 that were prepared. The gap in each bar represents the site of the deletion. The sequences of the oligonucleotides used in the inverse PCR are shown in their normal polarity or in the reversed polarity (*). The modified amino acid sequences and the numbering of the residues in the parent protein sequence are indicated below the bars.

MATERIALS AND METHODS

Viruses and cells. *Spodoptera frugiperda* (Sf9) cells were grown in suspension or monolayer cultures at 27°C in TNM-FH medium (JRH Biosciences) supplemented with 5% fetal calf serum and antibiotics. *Autographa californica* nuclear polyhedrosis virus recombinant derivatives were plaque purified and propagated in Sf9 cells as described elsewhere (20).

Deletion mutations of the CPV VP2 gene and construction of recombinant transfer vectors. Five regions of the VP2 gene of CPV were initially identified for deletion mutagenesis. Four of these regions were located at the tips of the four major loops of VP2. The other selected region was the amino terminus. The plasmid vector pCPV23, which contains the VP2 gene in the plasmid pMTL25, was used to manipulate the VP2 gene. Mutations in the amino terminus were prepared by direct PCR. The deletion mutations in the loops were created by inverse PCR (Fig. 1) (9). This PCR allows the creation of a deletion in a single step by amplification with two primers that have a corresponding gap between their 5′ ends. The primers are designed in inverted tail-to-tail directions to amplify the whole plasmid. The PCR product is then self-ligated, without further treatments. A prerequisite for a successful amplification is the previous linearization of the plasmid, using a unique restriction site within the region to be deleted. CPV VP2 gene contains unique *Hpa*I, *Spe*I, and *Mun*I restriction sites in the regions coding for loops 1, 2, and 4, respectively. For loop 3, a *Bfr*I restriction site was introduced by site-directed mutagenesis.

To make deletion Δ1 (loop 1, amino acids [aa] 88 to 99), *Hpa*I-digested pCPV23 was used as a template with forward primer D1(+) (nucleotides [nt] 298 to 318 [nucleotides are numbered from the initiation codon of the VP2 gene]) and back primer D1(−) (nt 261 to 242) (Table 1). The mutant PCR product was recovered and self-ligated by using the blunt ends. A new *Bfr*I restriction site was created in the deletions of the loops to allow the insertion of foreign sequences if necessary. This new site implies the creation of two new residues at positions 85 and 86 (Leu-Lys). The mutant was called pCPVΔ1.

For Δ2 (loop 2, aa 218 to 232), *Spe*I-digested pCPV23 was used as a template for forward primer D2(+) (nt 700 to 721) and back primer D2(−) (nt 651 to 631) (Table 1) to amplify a PCR product corresponding to the pCPV23 sequence containing the D2 deletion. Since this product showed blunt ends, it was self-ligated to generate mutant pCPVΔ2. Residues 235 and 236 were mutated to originate site *Bfr*I. The mutant was called pCPVΔ2.

For Δ3 (loop 3, aa 294 to 308), a site-directed mutagenesis was first carried out with pCPV13 to create a unique *Bfr*I restriction site. The USE mutagenesis was done according to previously described procedures (8). A unique *Afl*III restriction site was replaced by a *Bgl*II site by using the oligonucleotide CAGGAAA GAAGATCTGAGCAAAAG (nt 840 to 863 from pUC18) plus the oligonucleotide GAGCTACTAACTTAAGTGATATAGG (*Bfr*I sequence underlined). This protocol resulted in the inclusion of a new *Bfr*I site in loop 3. This new plasmid was called pCPV22. Next, forward primer D3(+) (nt 925 to 945) and back primer D3(−) (nt 879 to 859) (Table 1) were used with *Bfr*I-digested pCPV22 to make the PCR product, which was self-ligated to construct mutant pCPVΔ3.

For Δ4 (loop 4, aa 423 to 438), forward primer D4(+) (nt 1315 to 1334) and back primer D4(−) (nt 1266 to 1246) (Table 1) were used with *Mun*I-digested pCPV23 to make a PCR product corresponding to the required deleted VP2 sequence. This product was recovered and self-ligated to generate the mutant pCPVΔ4.

The three amino-terminal deletions were constructed by direct PCR with plasmid pCPV13 as a template and the oligonucleotide CPV1C (GTTAATATA ATTTTCTAGGTG) (nt 1756 to 1736) as a back primer (Table 1). Oligonucleotides CPVΔN9 (nt 13 to 34), CPVΔN14 (nt 28 to 49), and CPVΔN24 (nt 58 to 82) were used as forward primers to make the PCR products containing the required deletions. The PCR products were precipitated, phosphorylated, gel purified, and ligated into *Sma*I-digested pMTL25 to generate mutants pCPVΔN9, pCPVΔN14, and pCPVΔN24, respectively.

All of the deletion mutants of VP2 were rescued from the respective plasmids by *Bam*HI digestion and subcloned into the baculovirus transfer vector *Bam*HI-

TABLE 1. Oligonucleotides used for the construction of mutants

Mutant	Primers: Forward Name	Primers: Forward Sequence[a]	Primers: Back Name	Primers: Back Sequence
pCPVΔN9	CPVΔN9	*Bfr*I GCAGTTATGCTTAAGGGTGGTC	CPV1C	GTTAATATAATTTTCTAGGTG
pCPVΔN14	CPVΔN14	*Bfr*I GGTGGTATGCTTAAGGTCAGAA	CPV1C	
pCPVΔN24	CPVΔN24	*Bam*HI GCTACAGGATCCATGAACGGGTCTG	CPV1C	
pCPVΔ1	D1(+)	GATATTCATGCACAAATTGTA	D1(−)	*Bfr*I CATCTTAAGTACAACCACTC
pCPVΔ2	D2(+)	*Bfr*I CATCTTAAGGATCCAGATGATG	D2(−)	TGTTCTATCCCATTGAAAATA
pCPVΔ3	D3(+)	CAACAAGATAAAAGACGTGGT	D3(−)	*Bfr*I AGACTTAAGAAATGGTGGTAA
pCPVΔ4	D4(+)	AAAACAGGAATTAACTATAC	D4(−)	*Bfr*I AAGCTTAAGGTTAATATTTTG

[a] Nucleotides modified with respect to the original CPV sequence are indicated by dots. The new restriction sites are marked by lines.

digested pAcYM1 (16). The mutant sequences in the derived recombinant transfer vectors were confirmed by using the dideoxynucleotide procedure (19).

Insertion of foreign sequences into Δ2 mutant. To investigate the ability of Δ2 mutants to incorporate foreign sequences, the gonadotrophin-releasing hormone sequence was used as a model. Two oligonucleotides, TTAATGAACACTG GTCCTACGGACTACGGCCGGGAC (forward primer) and TTAAGTCCCG GCCGTAGTCCGTAGGACCAGTGTTCA (back primer), were allowed to self-anneal and ligated directly into the transfer vector pAcCPVΔ2 by using the *Bfr*I restriction site (underlined nucleotides correspond to the *Bfr*I recognition sequence).

PCRs. PCRs were performed with a Perkin-Elmer thermal reactor. Two types of PCRs were undertaken: inverse and direct, for deletions in the loops and the amino terminus, respectively.

For inverse PCR, 100 ng of DNA was mixed with 1.2 μg of primers and denatured for 3 min at 94°C. The samples were then subjected to 25 rounds of amplification under the following conditions: 93°C for 1 min, annealing at 40 to 45°C for 1 min, and extension at 72°C for 6 min (except for loop 1, 5.5 min). For direct PCR, 50 ng of template DNA was mixed with 800 ng of primers. The reaction conditions were similar except that the extension was for 2 min at 72°C. The reactions were done with Vent DNA polymerase (New England Biolabs), which leaves blunt ends in the PCR products.

Transfection and selection of recombinant viruses. *S. frugiperda* cells were transfected with a mixture of transfer plasmid DNA (2 μg) and linearized BacPak 6 (500 ng) as described by Kitts and Possee (11) in the presence of Lipofectin. After 5 to 6 days, culture supernatants were plated for baculovirus isolation in the presence of X-Gal (5-bromo-4-chloro-3-indolyl-β-D-galactopyranoside), white plaques were recovered, and the recombinant baculoviruses were plaque purified until high-titer virus stocks were obtained.

SDS-PAGE and immunoblotting analysis. *S. frugiperda* cells were infected with the different recombinant baculoviruses at a multiplicity of infection of 1 PFU per cell, and extracts of the cells were recovered at 72 h postinfection. Loading buffer was added to each cell extract or VLP preparation. The mixtures were heated at 100°C for 5 min, and the proteins were resolved by sodium dodecyl sulfate (SDS)–9% polyacrylamide gel electrophoresis (PAGE) and stained with Coomassie blue.

Proteins resolved by SDS-PAGE were electroblotted to a nitrocellulose membrane (Schleicher & Schuell) by using semidry equipment at 22 V for 45 min. The membrane was incubated for 1 h at room temperature in blocking buffer (3% skim milk in phosphate-buffered saline [PBS]). A mixture of CPV VP2-specific MAbs (14) was added and incubated for 2 h at room temperature. After washing, bound antibody was detected with alkaline phosphatase-conjugated goat anti-mouse immunoglobulin G antibodies (1:10,000 dilution in PBS) (Sigma). After washing, the color reaction was developed with BCIP (bromochloroindolyl phosphate) and nitroblue tetrazolium as substrates.

Purification of particles. *S. frugiperda* cells were infected with each recombinant baculovirus at a multiplicity of infection of 1 PFU per cell. Cells were harvested at 72 h postinfection, washed with PBS, and lysed at 4°C in 25 mM bicarbonate solution. Cell debris was removed by low-speed centrifugation. The particles in the extracts were then purified by 20% ammonium sulfate precipitation and centrifugation at 15,000 rpm for 15 min in an SS24 rotor (Sorvall). Sedimented particles were resuspended and dialyzed overnight against PBS. Particles were analyzed by SDS-PAGE and by negative-staining electron microscopy.

CsCl gradients. To determine if the mutant VP2 proteins expressed in insect cells assemble into capsids, cell extracts of infected cells were analyzed for their ability to band in CsCl gradients. To prepare the gradients, 0.5 ml of sample was added to 4.5 ml of a solution of CsCl at 1.3 g/cm^3 in Tris-EDTA buffer and centrifuged at 48,000 rpm for 24 h in a TST 55.5 rotor (Kontron). The gradients were fractionated, and each fraction was analyzed by SDS-PAGE and immunoblotting.

Electron microscopy analysis. To optimize the electron micrographs of individual samples, several dilutions and differential centrifugation steps were necessary: (i) VP2 extracts were diluted 1:3 in distilled water to obtain a suitable number of particles on the grid membrane, and all samples were stained and photographed at this dilution; (ii) the samples were then diluted 1:10 in distilled water and centrifuged at 3,000 × *g* for 5 min to remove large debris; and (iii) the supernatants were centrifuged at 30,000 × *g* for 20 min. The pellet thus formed was resuspended and stained and in some cases was ready for photography. The supernatant after this centrifugation was further centrifuged at 30,000 × *g* for 90 min. This pellet was resuspended, stained, and photographed in most cases. With this procedure, enhanced resolution can be obtained even from relatively crude samples.

To prepare the grids, they were placed on top of a drop of particle suspension for 10 min. The grids were rinsed by two transfers to a drop of distilled water. Negative staining was achieved by transfer of the grids to a drop of 2% uranyl acetate solution for 3 min. The grids were blotted from the edge and air dried. Microscopy and photography were performed on a Zeiss EM 10 instrument at 60 kV.

HA. HA analyses were carried out with a solution of 1% piglet erythrocytes according to previously described procedures (3).

RESULTS

Selection of domains of CPV VP2 that may be essential for VLP assembly. The CPV 64-kDa major capsid protein, VP2, is conserved among different parvoviruses of the Kilham's rat virus group. VP2 is arranged as trimers, which are the basis for the formation of virus capsids. The four loops of VP2, consisting of surface variable residues (Fig. 1) plus the amino terminus (Fig. 2), were targeted for deletion mutagenesis to determine whether mutations within these domains would abrogate

		1								9					14										24		
CPV VP2	TCCCC	**ATG**	**AGT**	**GAT**	**GGA**	**GCA**	**GTT**	**CAA**	**CCA**	**GAC**	**GGT**	**GGT**	**CAA**	**CCT**	**GCT**	**GTC**	**AGA**	**AAT**	**GAA**	**AGA**	**GCT**	**ACA**	**GGA**	**TCT**	**GGG**	**AAC**	**GGG**
		M	**S**	**D**	**G**	**A**	**V**	**Q**	**P**	**D**	**G**	**G**	**Q**	**P**	**A**	**V**	**R**	**N**	**E**	**R**	**A**	**T**	**G**	**S**	**G**	**N**	**G**
pCVP2ΔN9					TCCCC	**GCA**	**GTT**	**ATG**	**CTT**	**AAG**	**GGT**	**GGT**	**CAA**	**CCT**	**GCT**	**GTC**	**AGA**	**AAT**	**GAA**	**AGA**	**GCT**	**ACA**	**GGA**	**TCT**	**GGG**	**AAC**	**GGG**
								M	L	K	**G**	**G**	**Q**	**P**	**A**	**V**	**R**	**N**	**E**	**R**	**A**	**T**	**G**	**S**	**G**	**N**	**G**
pCVP2ΔN14									TCCCC		**GGT**	**GGT**	**ATG**	**CTT**	**AAG**	**GTC**	**AGA**	**AAT**	**GAA**	**AGA**	**GCT**	**ACA**	**GGA**	**TCT**	**GGG**	**AAC**	**GGG**
													M	L	K	**V**	**R**	**N**	**E**	**R**	**A**	**T**	**G**	**S**	**G**	**N**	**G**
pCVP2ΔN24																				TCCCC	**GCT**	**ACA**	**GGA**	**TCC**	**ATG**	**AAC**	**GGG**
																									M	**N**	**G**

FIG. 2. Diagrams of VP2 mutants with deletions in the amino terminus. The diagram at the top represents the nucleotide sequence corresponding to the first 26 aa of the unmodified CPV VP2. The other diagrams show the modified sequences of the deletion mutants that were prepared. When additional amino acids were inserted in lieu of the deletion, they are indicated in lightface.

the ability of VP2 to form VLPs. Deletion mutagenesis was chosen as a method for screening for important sequences in VP2 on the rationale that if particular amino acids within these sequences were required, then their removal would have a large effect on VLP formation. The longest sequences deleted consisted of 16 aa for loops 2 and 4 (Fig. 1) and 24 residues for the N terminus (Fig. 2). In the surface loops, no longer sequences were deleted, on the premise that large deletions would probably affect the overall structure of the protein in a nonspecific manner. In the amino terminus, the deletions were of 9, 14, and 24 aa to include the region containing the RNER domain and the 3C9 epitope, which are involved in virus neutralization and cell binding (7, 15, 25). It was thought that the N terminus could accommodate longer deletions, since it has shown a disordered structure and was thought not to play a major role in capsid morphogenesis or VLP formation. We have not included the glycine-rich region in the deletions, since it is well conserved in all of the autonomous parvoviruses, which suggests an essential role.

Residues in the amino terminus of VP2 essential for VLP formation. To construct each amino-terminal deletion mutant, a PCR was done with specific forward primers containing the mutated sequence in combination with a back primer annealing to the carboxy terminus of CPV VP2 (see Materials and Methods). The mutated genes were subcloned in the pAcYM1 baculovirus transfer vector and used to generate the recombinant baculoviruses. All of the derived recombinant baculoviruses expressed the deletion forms of the VP2 protein in insect cells (Fig. 3A, lanes ΔN9, ΔN14, and ΔN24). Compared with cell lysates from infections initiated with wild-type VP2 (Fig. 3A, lane CPV-VP2), all of the mutant viruses succeeded in making VP2 proteins with the molecular masses predicted by the amino acid sequences. However, the amounts of protein produced by each mutant were variable. ΔN9 and ΔN14 produced levels equal to or higher than that of normal CPV VP2. In contrast, the expressed ΔN24 was the only species that consistently showed lower levels of expression, which was probably due to less stability.

To determine whether the VP2 amino-terminal deletion mutants retained the ability to form VLPs, *S. frugiperda* cells were infected with each of the recombinant baculoviruses that made a mutant VP2 protein (ΔN9, ΔN14, and ΔN24), at a multiplicity of infection of 1 PFU per cell. The baculovirus expressing the unmodified VP2 protein served as a control. Infected cells were collected 3 days postinfection and lysed by osmotic shock. The three amino-terminal mutants were precipitated by a low (20%) ammonium sulfate concentration, which is a first indication for a particular or supramolecular nature. Lysates of infected insect cells expressing the proteins were analyzed in CsCl gradients. In the three mutants an opalescent band indicative of VLP presence could be seen. However, when the density was determined, the ΔN24 mutant banded at a density slightly lower (1.28 g/cm^3) than that for VLPs or normal empty CPV capsids (1.33 g/cm^3). The material recovered from the gradient bands was analyzed by immunoblotting (Fig. 3B, lanes ΔN9, ΔN14, and ΔN24). In all of the mutants, a VP2 was observed, although in the case of mutant ΔN24 the intensity of the band was much lower. SDS-PAGE analyses of recovered materials from these gradients showed a broad distribution of the VP2 on the upper part of the gradient, suggesting the presence of monomers or incomplete particles in the preparations.

Electron microscopy analyses confirmed the formation of regular VLPs in mutants ΔN9 (Fig. 4B) and ΔN14 (Fig. 4C) but not in ΔN24 (Fig. 4D). ΔN24 particles showed an incorrect capsid assembly, with some type of aggregation or multimeric structure but forming completely irregular particles morphologically very different from regular VLPs. In agreement with these data, the mutant ΔN24 had lost the ability to hemagglutinate piglet erythrocytes. The other two mutants retained the HA properties, although with titers lower than those of normal VLPs. From these data, it was concluded that some portion of the sequence between residues 14 and 24 was essential for correct VLP formation.

Expression of four mutant VP2 proteins with deletions in the loops. The four loops of VP2 were investigated for their roles in VLP formation by deletion of the sequences at the tips of the loops. These tips are located in residues 92 and 93, 222 and 223, 300 to 303, and 421 to 443 for loops 1, 2, 3 and 4, respectively, and are on the extreme outside surface of the virus (24). Deletions were located in positions 88 to 99, 218 to 233, 294 to 308, and 423 to 438, respectively. These regions were selected on the rationale that together with equivalent structures from two other threefold-related subunits they make up the threefold spikes, which play a highly relevant role for many virion properties.

To construct the chimeric genes and since no unique restriction sites were available, the fastest strategy was to perform inverse PCR (9), which avoids cloning steps and allows recovery of functional clones in a single step, by self-ligation only. The chimeric genes were isolated from the cloning vector and subcloned into pAcYM1. Four recombinant baculoviruses ex-

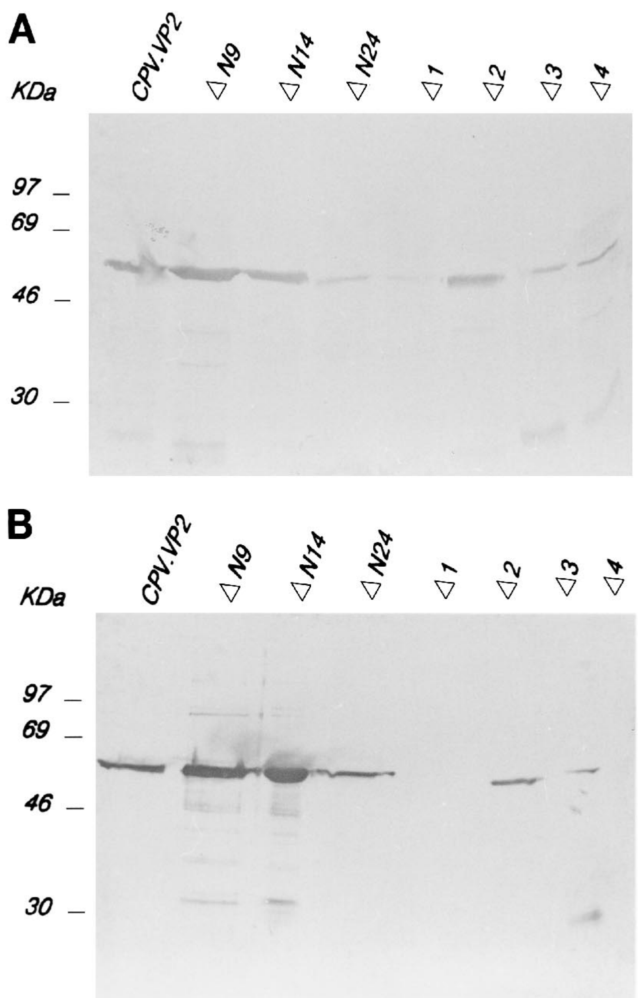

FIG. 3. Expression and formation of empty capsids by the VP2 deletion mutants in insect cells. *S. frugiperda* cells were infected with each recombinant baculovirus at a multiplicity of infection of 1 PFU per cell. Extracts of the cells were harvested at 72 h postinfection and prepared as described in Materials and Methods. (A) After treatment with loading buffer, proteins were resolved by SDS-PAGE, transferred to nitrocellulose membranes, and reacted with a mixture of CPV-specific MAbs in Western blot (immunoblot) analysis. The different deletion mutants used are indicated above the lanes. CPV-VP2, wild-type CPV VP2. In the preparations corresponding to mutants Δ3 and Δ4, other, low-molecular-mass fragments of VP2, which probably reflect degradation products of the expressed proteins, appear. (B) Cell extracts were subjected to isopycnic centrifugation in CsCl gradients. The material recovered from the fractions corresponding to the density of empty capsids in CsCl gradients was assessed by immunoblotting with anti-CPV MAbs and alkaline phosphatase-conjugated goat anti-mouse immunoglobulin G. The positions of the different deletion mutants are indicated. CPV-VP2, wild-type CPV VP2. No detectable peaks were observed for Δ1 and Δ4.

pressing each mutant with deletions in the four loops of CPV VP2 were generated. The expression of the modified proteins was identified by SDS–9% PAGE and immunoblotting analysis of extracts of infected insect cells. By comparison with a recombinant that expresses the unmodified VP2 protein, four proteins of slightly smaller size were identified in the blotting analysis of insect cells (Fig. 3A, lanes Δ1 to Δ4). Like unmodified VP2 (Fig. 3A, lane CPV-VP2), the deletion mutants of VP2 were recognized by MAb 3C9 (Fig. 3A, lanes Δ1 to Δ4). Mutant Δ2 showed the fastest migration for unknown reasons. With similar experimental infection conditions, lower yields of VLPs with respect to that for the wild type were routinely observed for all of the mutants, except for mutant Δ2, which showed similar or higher levels of expression. Immunoblotting of mutants Δ3 and Δ4 showed the presence of a larger proportion of shorter VP2 molecules, suggesting a proteolytic degradation of VP2 as a consequence of a lower stability. This is a first indication of the absence of particles in these preparations. A second indication came from the ammonium sulfate precipitation, in which only the Δ2 mutant precipitated well, Δ1 and Δ3 precipitated partially, and Δ4 did not precipitate at all. Finally, when the different preparations were analyzed for HA, the mutants with mutations in loops 1, 3, and 4 had lost this property. Only loop 2 remained able to hemagglutinate piglet erythrocytes, although with lower titers than normal VLPs.

Effect of deletions in the loops on the formation of VLPs. To examine whether the chimeric VP2 would assemble to form VLPs, *S. frugiperda* cells were infected with each recombinant baculovirus, and the particles were purified as described above and observed visually in CsCl gradients. From the isopycnic centrifugation, mutants Δ2 and Δ3 gave rise to visible bands, with a density of 1.33 g/cm^3. When these gradients were fractionated and analyzed by immunoblotting, only in those fractions of mutants Δ2 and Δ3 corresponding to densities of 1.28 to 1.33 g/cm^3 were the expected proteins observed (Fig. 3B, lanes Δ1 to Δ4). Thus, it seemed that mutants Δ2 and Δ3 were competent to make particles despite the deleted sequences, whereas mutants Δ1 and Δ4 were not.

A final assessment of the VLP formation by these mutants was done by electron microscopy. When these preparations were observed by electron microscopy (Fig. 4), only those corresponding to Δ2 showed a morphology similar to that of the regular VLPs (Fig. 4E). Mutant Δ3, although banding in the CsCl gradients, showed an irregular morphology very different from that of VLPs, suggesting that there is some type of aggregation but not a proper assembly of the capsids (Fig. 4F). In the other two mutants, Δ1 and Δ4, no aggregation or particulate structure was observed.

Do deletions in loop 2 allow the insertion of foreign epitopes retaining the ability to form VLPs? It was previously demonstrated that porcine parvovirus VLPs expressed in insect cells can incorporate foreign epitopes in the unmodified amino terminus of VP2 (20). In view of the potential application of these VLPs as platforms for the presentation of foreign epitopes, it was of interest to determine whether mutants with deletions in loop 2 were also permissive for the insertion of foreign sequences. A sequence corresponding to the gonadotrophin-releasing hormone, 12 aa long, was inserted into the loop 2 deletion mutant, taking advantage of the unique *Bfr*I restriction site newly introduced in pCPVΔ2.

The modified protein was expressed at levels similar to those of the original Δ2 mutant. It was recognized by MAb 3C9, precipitated with ammonium sulfate, and formed an opalescent band in CsCl gradients (data not shown). Electron microscopy analysis showed the presence of large numbers of protein aggregates with a size and morphology similar to those of the original VLPs (Fig. 5). However, an unusual feature observed in these preparations was the presence of some partially broken capsids, which is indicative of difficulties in capsid assembly. The presence of regular VLPs makes these chimeric capsids attractive candidates for antigen delivery.

DISCUSSION

The major CPV capsid protein, VP2, assembles into virus-like structures independently of the presence of other virion

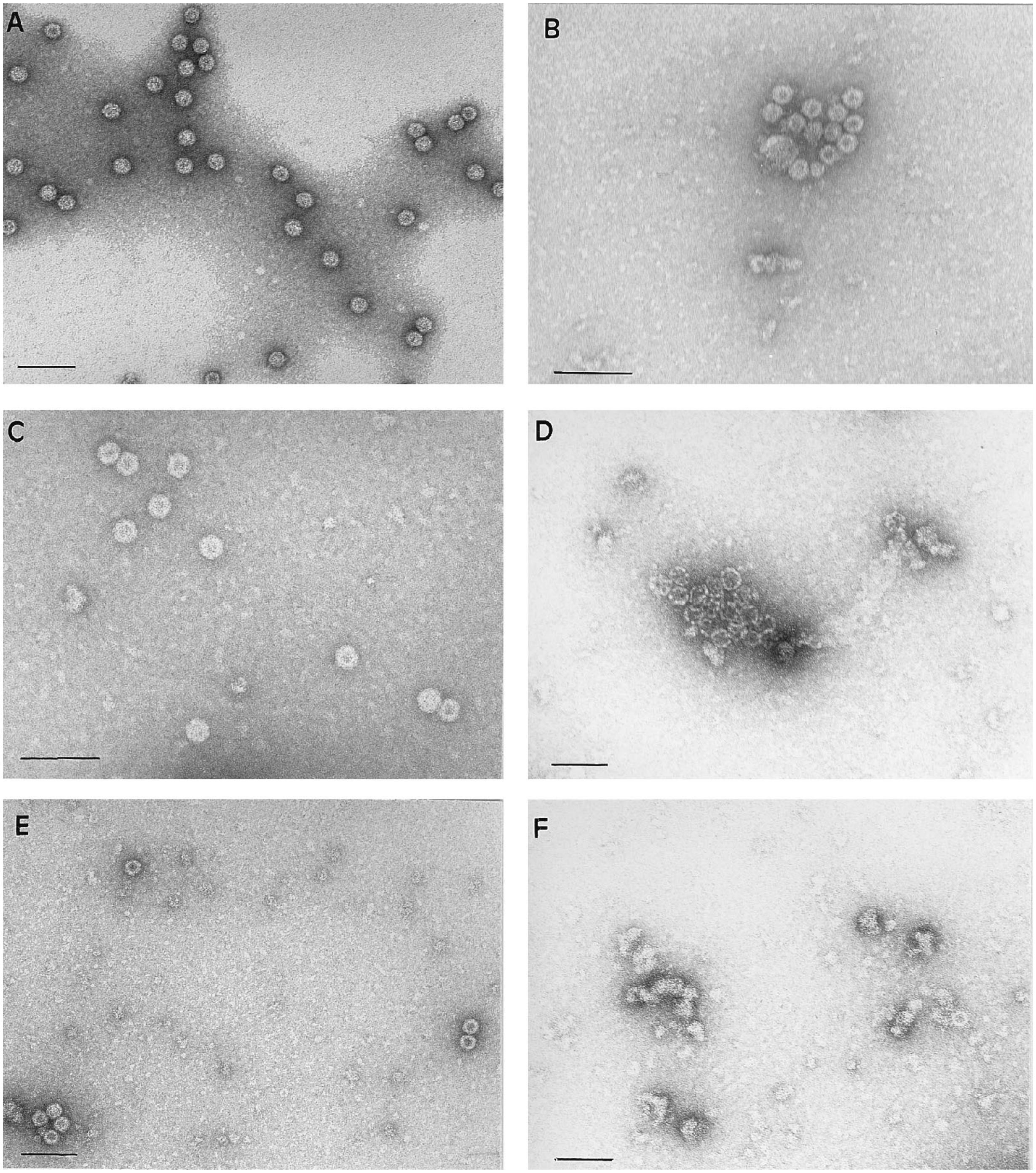

FIG. 4. Electron microscopy. Purified wild-type VP2 (A), ΔN9 (B), ΔN14 (C), ΔN24 (D), Δ2 (E), and Δ3 (F) preparations were negatively stained and observed by electron microscopy. Bars, 100 nm.

proteins or viral DNA. This property has allowed us to establish a functional assay for identifying regions of VP2 necessary for capsid formation. In this study, we have generated mutants of VP2 with deletions in the amino terminus and surface loops, which were subsequently expressed by recombinant baculoviruses. Using this approach, we defined two nonessential regions for CPV capsid assembly. These regions are located in the first 14 residues of the amino terminus and on the tip of loop 2. Other regions, such as loops 1, 3, and 4, plus sequences beyond the first 15 aa of the amino terminus, were shown to be essential for VLP formation. Recently, we have applied a similar system to study the role of the carboxy terminus and the effect of insertions in the amino terminus in the formation of porcine parvovirus VLPs (20). Direct insertions, up to 17 aa, in the amino terminus did not alter the capsid formation and demonstrated the internal position of the amino terminus in empty capsids. In contrast, mutants with deletions in the carboxy terminus showed that this domain was also essential for

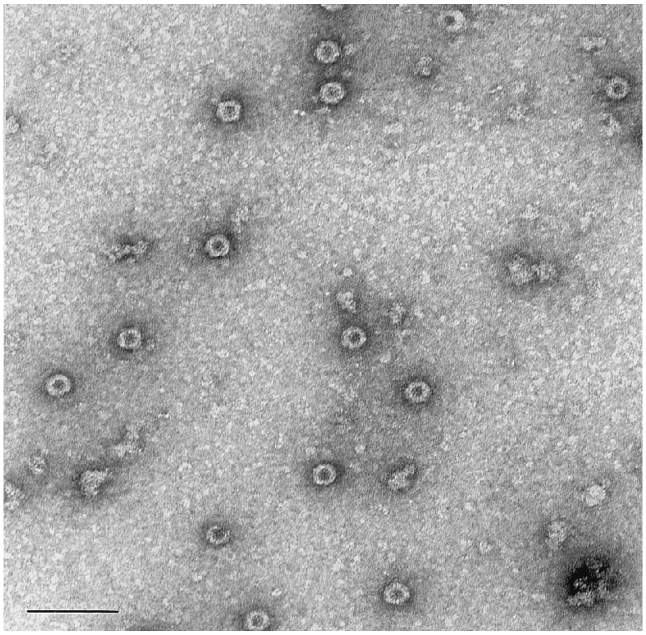

FIG. 5. Electron microscopy analysis of negatively stained preparations of Δ2 with an insertion of a gonadotrophin-releasing hormone sequence. Bar, 100 nm.

VLP formation. Because of the genetic similarity of the two viruses, we anticipate that the results obtained with porcine parvovirus could be extrapolated to CPV. For porcine parvovirus VLPs, the lack of a known three-dimensional structure and appropriate restriction sites in the putative loop sequences makes the generation of deletion mutations in those areas selected for this report more difficult.

The disorder of the amino termini of CPV VP2 was assumed to be due to association of this region with the viral DNA (10). For this reason, no participation of the amino-terminal domain in capsid conformation and morphogenesis was expected. This presumption was examined by preparing three mutants with deletions in the amino terminus. The first two of these mutants, ΔN9 and ΔN14, were able to assemble into normal VLPs. However, residues 14 to 24 (deleted in ΔN24) were found to be critical for VLP formation, affecting in some manner the stability or efficiency of formation of the particles. In ΔN24, the binding motif of neutralizing MAb 3C9 and the RNER cell binding domain are lost. Previous immunofluorescence data (7) suggested a potential role for this region in capsid assembly and a possible interference of MAb 3C9 in the process of decapsidation of the virus after attachment to the cell. Here we confirm the relevance of this region in capsid assembly and morphogenesis. In contrast to our results, recent findings for B19 (10) have shown that most of the amino terminus (up to 25 aa), including the polyglycine region, can be removed without affecting capsid self-assembly. These differences are more significant if we consider that in B19 the amino terminus adjacent to the glycine-rich region is much shorter and the polyglycine region, located between aa 12 and 17, is within the initial 25 residues that can be deleted. Therefore, the requirements for capsid assembly seem to be very different for B19 and the Kilham's rat group of parvoviruses.

Regarding deletions in the loops, there was a considerable effect on the capability of VP2 to assemble after the selected regions were deleted, which agrees with previous observations on the relevance of these loops in antigenicity, binding of neutralizing antibodies, host range differentiation, pathogenicity, and HA. Three types of morphology were found: normal VLPs (loop 2), VP2 aggregates (loop 3), and no interaction at all between monomers (loops 1 and 4). Deletion of residues 218 to 233 (Δ2) had no effect on VLP formation, demonstrating this sequence to be nonessential for virus assembly. The nature of the aggregates in Δ3 mutants is not easy to understand. A similar phenomenon is observed also in ΔN24 mutants, although the morphology was different in both cases. It is not clear if they represent an intermediate state in capsid assembly. In any case, they showed a lower density and are much more unstable than regular VLPs. The results obtained with loop 4 were remarkable. On the one hand, the large intertwining of this loop in the formation of the spike of the parvovirus capsid and VP2-VP2 interactions (24, 26) probably makes this region nonpermissive for modifications. On the other hand, the results are surprising in that the large size of loop 4 would be enough for accepting modifications without disrupting the structure. The effect of the deletions in loop 1 is somewhat unexpected, because it is less involved in subunit interactions than the other two loops (26). Probably this mutation affects the folding of VP2, which results in no assembly of the VLPs. From our results, it seems evident that there is a clear relationship between assembly, stability, and levels of production of mutant VP2 molecules. In those cases in which VP2 does not assemble into particles, it seems to be less stable and more prone to quick degradation. In contrast, the loop 2 mutant was obtained at levels similar to or higher than those of the wild type.

At the same time, we examined the deletion mutants for their abilities to hemagglutinate. HA of pig erythrocytes is a property of wild-type isolates of CPV and VP2 VLPs, being in general a good marker for particle formation. In a previous report (22), the essential role of the "dimple" region in erythrocyte binding was demonstrated. Here we demonstrate that deletions in loops 1, 3, and 4 are associated with loss of HA. The most likely explanation is that these deletions have caused extensive alterations in the structure and process of capsid assembly. Loop 2 seems not to be implicated so strongly in the HA process.

A further extension of this research was to investigate whether these loops can tolerate additional sequences introduced by direct insertions, which would make these capsids interesting platforms for the presentation of foreign antigens. Since loop 2 forms part of antigenic site A (21), it could be a suitable candidate for epitope presentation and antigen delivery. The experiments with Δ2 mutants confirmed the promising feature of self-assembly and correct exposure of the epitope on the surface of the capsid. From these results and previous data on porcine parvovirus VLPs (20), we can conclude that only a few sites within VP2, i.e., the amino terminus and/or loop 2, will allow deletions or insertions of foreign epitopes for use in antigen delivery. To complete these studies, further research will address the construction of new mutants containing insertions in the four loops to determine if these loops are more tolerant to insertion of sequences than to deletions.

ACKNOWLEDGMENTS

A. Hurtado is a recipient of a fellowship of the Spanish Ministry of Education and Science. This work was partially supported by an EU grant (EEC Biotechnology B102-CT92-0290).

We thank Kristian Dalsgaard and Jan Langeveld for helpful discussion and a critical review of the manuscript.

REFERENCES

1. **Ball-Goodrich, L. J., and P. Tattersal.** 1992. Two amino acid substitutions within the capsid are coordinately required for acquisition of fibrotropism by the lymphotropic strain of minute virus of mice. J. Virol. **66:**3415–3423.
2. **Bloom, M. E., S. Alexandersen, C. Garon, S. Mori, W. Wei, S. Perryman, and J. B. Wolfinbarger.** 1988. Nucleotide sequence and genomic organization of Aleutian mink disease parvovirus (ADV): sequence comparisons between a nonpathogenic and a pathogenic strain of ADV. J. Virol. **62:**2903–2915.
3. **Carmichael, L. E., J. C. Joubert, and R. Pollock.** 1980. Hemagglutination by canine parvovirus: serologic studies and diagnostic applications. Am. J. Vet. Res. **4:**784–791.
4. **Casal, J. I., J. P. M. Langeveld, E. Cortés, W. W. M. Schaaper, E. van Dijk, C. Vela, S. Kamstrup, and R. H. Meloen.** 1995. Peptide vaccine against canine parvovirus: identification of two neutralization subsites in the N terminus of VP2 and optimization of the amino acid sequence. J. Virol. **69:**7274–7277.
5. **Chang, S. F., J. Y. Sgro, and C. R. Parrish.** 1992. Multiple amino acids in the capsid structure of canine parvovirus coordinately determine the canine host range and specific antigenic and hemagglutination properties. J. Virol. **66:** 6858–6867.
6. **Chapman, M. S., and M. G. Rossmann.** 1993. Structure, sequence and function correlations among Parvoviruses. Virology **194:**491–508.
7. **Cortés, E., C. Sanmartin, J. Langeveld, R. Meloen, K. Dalsgaard, C. Vela, and J. I. Casal.** 1993. Topographical analysis of canine parvovirus virions and recombinant VP2 capsids. J. Gen. Virol. **74:**2005–2010.
8. **Deng, W. P., and J. A. Nickoloff.** 1992. Site-directed mutagenesis of virtually any plasmid by eliminating a unique site. Anal. Biochem. **200:**81–88.
9. **Imai, Y., Y. Matsushima, T. Sugimura, and M. Terada.** 1991. A simple and rapid method for generating a deletion by PCR. Nucleic Acids Res. **19:**2785.
10. **Kawase, M., M. Momoeda, N. S. Young, and S. Kajigaya.** 1995. Modest truncation of the major capsid protein abrogates B19 parvovirus capsid formation. J. Virol. **69:**6567–6571.
11. **Kitts, P. A., and R. D. Possee.** 1993. A method for producing recombinant baculovirus expression vectors at high frequency. BioTechniques **14:**810–817.
12. **Langeveld, J., J. I. Casal, A. D. M. Osterhaus, E. Cortés, R. Swart, C. Vela, K. Dalsgaard, W. C. Puijk, W. M. Schaaper, and R. H. Meloen.** 1994. First peptide vaccine providing protection against viral infection in the target animals: studies of canine parvovirus in dogs. J. Virol. **68:**4506–4513.
13. **Langeveld, J., J. I. Casal, C. Vela, K. Dalsgaard, S. H. Smale, W. C. Puijk, and R. H. Meloen.** 1993. B-cell epitopes of canine parvovirus: distribution on the primary structure and exposure on the viral surface. J. Virol. **67:**765–772.
14. **Lopez de Turiso, J. A., E. Cortés, C. Martinez, R. Ruiz de Ybañez, I. Simarro, C. Vela, and J. I. Casal.** 1992. Recombinant vaccine for canine parvovirus in dogs. J. Virol. **66:**2748–2753.
15. **Lopez de Turiso, J. A., E. Cortés, A. Ranz, J. Garcia, A. Sanz, C. Vela, and J. I. Casal.** 1991. Fine mapping of canine parvovirus B cell epitopes. J. Gen. Virol. **72:**2445–2456.
16. **Matsuura, Y., R. D. Possee, H. A. Overton, and D. H. L. Bishop.** 1987. Baculovirus expression vectors: the requirements for high level expression of proteins, including glycoproteins. J. Gen. Virol. **68:**1233–1250.
17. **Rossmann, M. G., and J. E. Johnson.** 1989. Icosahedral RNA virus structure. Annu. Rev. Biochem. **58:**533–573.
18. **Saliki, J. T., B. Mizak, H. P. Flore, R. R. Gettig, J. P. Burand, L. E. Carmichael, H. A. Wood, and C. R. Parrish.** 1992. Canine parvovirus empty capsids produced by expression in a baculovirus vector: use in analysis of viral properties and immunization of dogs. J. Gen. Virol. **61:**33–41.
19. **Sanger, F., S. Nicklen, and A. R. Coulson.** 1977. DNA sequencing with chain-terminating inhibitors. Proc. Natl. Acad. Sci. USA **74:**5463–5467.
20. **Sedlik, C., J. Sarraseca, P. Rueda, C. Leclerc, and J. I. Casal.** 1995. Immunogenicity of poliovirus B and T cell epitopes presented by hybrid porcine parvovirus particles. J. Gen. Virol. **76:**2361–2368.
21. **Strassheim, M. L., A. Gruenberg, P. Veijalainen, J. Y. Sgro, and C. R. Parrish.** 1994. Two dominant neutralizing antigenic determinants of Canine Parvovirus are found on the threefold spike of the virus capsid. Virology **198:**175–184.
22. **Tresnan, D. B., L. Southard, W. Weichert, J. Y. Sgro, and C. R. Parrish.** 1995. Analysis of the cell and erythrocyte binding activities of the dimple and canyon regions of the canine parvovirus capsid. Virology **211:**123–132.
23. **Truyen, U., M. Agbandje, and C. R. Parrish.** 1994. Characterization of the feline host range and a specific epitope of Feline Panleukopenia Virus. Virology **200:**494–503.
24. **Tsao, J., M. S. Chapman, M. Agbandje, W. Keller, K. Smith, H. Wu, M. Luo, T. J. Smith, M. G. Rossmann, R. W. Compans, and C. R. Parrish.** 1991. The three dimensional structure of canine parvovirus and its functional implications. Science **251:**1456–1464.
25. **Tullis, G. E., L. R. Burger, and D. J. Pintel.** 1992. The trypsin sensitive RVER domain in the capsid proteins of Minute Virus of Mice is required for efficient cell binding and viral infection but not for proteolytic processing *in vivo*. Virology **191:**846–857.
26. **Wu, H., and M. G. Rossmann.** 1993. The canine parvovirus empty capsid structure. J. Mol. Biol. **233:**231–244.